Molecular Vision 2022; 28:507-515 <http://www.molvis.org/molvis/v28/507>
Received 14 January 2022 | Accepted 29 December 2022 | Published 31 December 2022

PET imaging of retinal inflammation in mice exposed to blue light using [^{18}F]-DPA-714

Yuan Chen,[1] Yixiang Zhou,[1] Xue Zhu,[1,2] Ge Yan,[1] Donghui Pan,[2] Lizhen Wang,[2] Min Yang,[1,2] Ke Wang[1,2]

[1]Department of Radiopharmaceuticals, School of Pharmacy, Nanjing Medical University, Nanjing, Jiangsu Province, China; [2]NHC Key Laboratory of Nuclear Medicine, Jiangsu Key Laboratory of Molecular Nuclear Medicine, Jiangsu Institute of Nuclear Medicine. Wuxi, Jiangsu Province, China

Purpose: Positron emission tomography (PET) is widely used in high-precision imaging, which may provide a simple and noninvasive method for the detection of pathology and therapeutic effects. [^{18}F]-DPA-714 is a second-generation translocator protein (TSPO) positron emission tomography radiotracer that shows great promise in a model of neuroinflammation. In this study, [^{18}F]-DPA-714 micro-PET imaging was used to evaluate retinal inflammation in mice exposed to blue light, a well-established model of age-related macular degeneration (AMD) for molecular mechanism research and drug screening.

Methods: C57BL/6J melanized mice were subjected to 10,000, 15,000, and 20,000 lux blue light for 5 days (8 h/day) to develop the retinal injury model, and the structure and function of the retina were assessed using hematoxylin–eosin (HE) staining, electroretinography (ERG), and terminal-deoxynucleotidyl transferase (TdT)-mediated nick-end labeling (TUNEL) immunostaining. Then, [^{18}F]-DPA-714 was injected approximately 100 µCi through each tail vein, and static imaging was performed 1 h after injection. Finally, the mice eyeballs were collected for biodistribution and immune analysis.

Results: The blue light exposure significantly destroyed the structure and function of the retina, and the uptake of [^{18}F]-DPA-714 in the retinas of the mice exposed to blue light were the most significantly upregulated, which was consistent with the biodistribution data. In addition, the immunohistochemical, western blot, and immunofluorescence data showed an increase in microglial TSPO expression.

Conclusions: [^{18}F]-DPA-714 micro-PET imaging might be a good method for evaluating early inflammatory status during retinal pathology.

Age-related macular degeneration (AMD) is a chronic and progressive degenerative disease of the retina that culminates in blindness and mainly affects the elderly population. AMD shows a high prevalence, with a distinct trend of increase: About 10%–20% of people over the age of 65 suffer from maculopathy (an early stage) or overt macular degeneration [1-4]. RPE and photoreceptor degeneration over time in the macular area are characteristics of AMD [5]. Most of the strategies for preserving visual function have been developed in animal models. Age, smoking, genetic factors, and exposure to sunlight have been identified as risk factors for the development of AMD [6]. Within the solar spectrum, blue light is more highly involved in disease induction; thus, animals exposed to blue light are estimated to be a well-established model of AMD for molecular mechanism research and drug screening, where it affords high reproducibility, rapid induction, ease of use, and flexibility through modulation of light duration and intensity [7,8].

Correspondence to: Ke Wang, NHC Key Laboratory of Nuclear Medicine, Jiangsu Key Laboratory of Molecular Nuclear Medicine, Jiangsu Institute of Nuclear, Qiangrong Road 20, Wuxi, Jiangsu Province, China, 214063, Phone: +86 (510) 85514482; email: wangke@jsinm.org

Positron emission tomography (PET) is a sensitive and specific functional imaging method that allows metabolic mapping of disease processes in humans. Compared to other imaging methods, the most extensive application of micro-PET imaging to small animal models of disease is in the area of cancer biology [9]. However, with the discovery and synthesis of more imaging targets and imaging agents, the application of PET in other disciplines is gradually expanding, such as in the heart, brain, and lung. Some imaging agents have also been developed in the eye [10-12]. Among them, the 18 kDa translocator protein (TSPO) ligand as the imaging agent of PET imaging technology plays an important role in the diagnosis and treatment of neurodegenerative diseases, such as Alzheimer's disease and cerebral ischemia [13-16]. TSPO (translocator protein) is an evolutionarily conserved outer mitochondrial membrane (OMM) protein highly expressed in activated microglia, and TSPO-targeting PET imaging is used for the evaluation of neuroinflammation. It has been reported that TSPO exogenous ligands are also important markers in patients with AMD [17]. [^{18}F]-DPA-714, a targeted radiotracer for TSPO, has been used for imaging nervous system diseases caused by microglia activation [18,19]. The application of [^{18}F]-DPA-714 to the rat model

of diabetic retinopathy (DR) was recently reported [20]. However, there is no study on the application of [^{18}F]-DPA-714 in the AMD animal model. Based on the study above, [^{18}F]-DPA-714 micro-PET imaging was chosen in the mouse model with blue light irradiation to evaluate the value of noninvasive methods in identifying retinal inflammation of AMD.

METHODS

Animals and ethics statement: A cohort of 4- to 6-week-old C57BL/6J mice (ChangZhou Cavens, Laboratory Animal Co., Ltd, Changzhou, China) were used for the experiments, which were raised in a 12 h:12 h light-dark cycle of 5 lux white light with free access to food and water. Age-matched mice were randomly assigned to the blue light damage (BL) and control (non-light damage) groups (n = 3 per group). Animals in the blue light damage group were exposed to 10–20 k lux blue LED light (OcuTech, Wuxi, China) for 5 days (8 h/day, from 09:00 to 17:00). The pupils were dilated twice daily at 10:00 and 18:00 with a single drop of 1% atropine sulfate (8.3 mg of atropine). The pupils of the control animals were also dilated twice each day and were returned to dim cyclic light (12 h:12 h light-dark cycle, 5 lux). A custom light box was constructed for free adjustment of light intensity and time. All animal experiments in this study were approved by the Laboratory Animal Management and Ethics Committee of the Jiangsu Institute of Nuclear Medicine and which adhered to the Association for Research in Vision and Ophthalmology (ARVO) statement for the use of animals in ophthalmic and vision research.

Hematoxylin–eosin staining: Immediately after blue light exposure, an overdose of sodium pentobarbital was injected, and the eyeballs of the mice in the different groups were immediately removed and embedded in paraffin blocks. Then, 5 μm paraffin sections were used for hematoxylin–eosin (HE) staining. After deparaffinization, hydration, HE staining, dehydration, transparency, and other steps, the slides were observed under a microscope (Nikon, Tokyo, Japan). Briefly, after deparaffinization and rehydration, 5 μm longitudinal sections were stained with hematoxylin solution for 5 min followed by 5 dips in 1% acid ethanol (1% HCl in 70% ethanol) and then rinsed in distilled water. Then the sections were stained with eosin solution for 3 min and followed by dehydration with graded alcohol and clearing in xylene.

Electroretinography: All animals were dark adapted for at least 12 h before the electroretinography (ERG) recording. Under dim red light, the mice were anesthetized with tail vein injection of ketamine (80 mg/kg) and xylazine (10 mg/kg). The vessels were dilated with topical 0.5% tropicamide and 0.5% phenylephrine hydrochloride. The corneas were kept moist with methylcellulose solution. A gold wire was placed on the moistened cornea as the recording electrode, and a gold reference electrode was placed in the mouth. Simultaneous recordings were made from both eyes at a bandwidth of 0.1–500 Hz with a needle electrode inserted close to the tail. Dark-adapted ERGs were elicited with a series of white single flash stimuli from −4.8 to 2.25 log CD-s/m^2. A-wave amplitude was measured from the prestimulus baseline to the initial negative trough at intensities ranging from −1.8 to 2.25 log CD-s/m^2 flashes. B-wave amplitudes were measured from the baseline or the a-wave, if present, to the peak of flashes with intensities of −4.8 to 0.3 logCD-s/m^2. Photoreceptor functional changes were evident from averaging the a- and b-wave amplitudes for each intensity.

Immunofluorescence: To detect apoptotic cells in the retina, terminal-deoxynucleotidyl transferase (TdT)-mediated mediated nick-end labeling (TUNEL) immunostaining (Beyotime, Nantong, China) was employed to evaluate apoptotic cells in the retina. Frozen retinal sections were stained using a Cy3 labeling fluorometric TUNEL system and then mounted with 2-(4-Amidinophenyl)-6-indolecarbamidine dihydrochloride (DAPI; Beyotime, Nantong, China). To verify the expression and location of TSPO in the retina, colocalization of TSPO (1:500, cat. no. ab109497, Abcam,Cambridge, MA) and microglial marker IBA-1 (1:500, cat. no. ab283319, Abcam) was conducted. Frozen retinal sections were randomly selected and stained with TSPO/IBA-1/DAPI antibodies overnight (36–48 h) at 4 °C in a humidified box. The sections were then incubated with fluorescence-labeled secondary antibodies (1:250, goat anti-rabbit FITC-labeled IgG (H+L) Alexa Fluor 647-labeled IgG (H+L), cat. no. ab6717, Abcam; goat anti-mouse IgG H&L-Alexa Fluor 647, cat. no. ab150115, Abcam) for 2 h at 4 °C in a humidified box. After washing and air drying, the slides were blocked using PBS/glycerol (1X; 120 mM NaCl, 20 mM KCl, 10 mM $NaPO_4$, 5 mM KPO_4, pH 7.4) for observation under a fluorescence microscope (Nikon, Tokyo, Japan).

Micro-PET image and biodistribution: [^{18}F]-DPA-714 was synthesized as previously described [21], and the radiochemical purity was >98%. Under anesthetization, the mice were injected intravenously with 3.7 MBq [^{18}F]-DPA-714, and static micro-PET imaging was performed for 10 min at 1 h post-injection. Data were analyzed using the reported method [22]. After micro-PET imaging, the mice were euthanized by intraperitoneal injection of pentobarbital sodium (200 mg/kg), and major organs were extracted. The eyeballs were dissected as the cornea, vitreous body, retina, and choroid. All organs were collected and weighed. Radioactivity in the

tissues was measured using a γ-counter, and uptake values were expressed as % ID/g.

Immunohistochemistry: Eyeballs were immersed in 4% paraformaldehyde for 4 h and transferred to 70% ethanol. Individual lobes of eyeball biopsy material were placed in processing cassettes, dehydrated through a serial alcohol gradient, and embedded in paraffin. Before immunohistochemistry (IHC), 5 μm thick eyeball tissue sections were dewaxed in xylene, rehydrated through decreasing concentrations of ethanol, and washed in PBS. Then, they were stained with TSPO antibody (1:500, cat. no. ab109497, Abcam) and hematoxylin. After staining, the sections were hydrated with increasing concentrations of ethanol and xylene. The next day, the slides were rinsed and incubated with the corresponding secondary antibody (Beyotime, Nantong, China) for 30 min followed by 3,3′-diaminobenzidine (DAB) and hematoxylin staining, respectively. The slides were then observed under a microscope (Nikon, Tokyo, Japan).

Western blotting: Western blotting was used to identify the expression level of TSPO protein. Tissues were ground and lysed in radio-immunoprecipitation assay (RIPA) buffer. The concentration of protein was assessed with a bicinchoninic acid (BCA) assay. Then, the protein of each sample was loaded onto 12% sodium dodecyl sulfate polyacrylamide gel electrophoresis (SDS–PAGE) and transferred onto polyvinylidene fluoride (PVDF)membranes. The membranes were blocked with 5% nonfat milk and then incubated with the primary antibody (TSPO, 1:1,000, cat. no. ab109497, Abcam), followed by the secondary antibody (goat anti-rabbit IgG H&L-HRP, 1:500, cat. no. ab6721, Abcam). The protein bands were visualized using the enhanced chemiluminescence (ECL) assay kit. The density of each band was normalized to the expression of glyceraldehyde-3-phosphate dehydrogenase (GAPDH; 1:1000, cat. no. ab9485, Abcam).

Statistical analysis: GraphPad Prism V:6.01 software was used for the statistical analysis. The data are expressed as the means ± standard error of mean (SEM). Statistical comparisons were conducted with the Student *t* test between two groups and one-way ANOVA followed by Tukey's post hoc test among three groups. P values of less than 0.05 were considered statistically significant.

RESULTS

Blue light exposure destroys the structure of the retina: To investigate the influence of blue light exposure on the retinal structure, the mice were exposed to blue light for 5 days (8 h/day), and HE staining of the retina was performed. Light intensities of 10,000, 15,000, and 20,000 lux were chosen. Five days after modeling, HE staining showed that the structure of each layer in the retinas of the control mice was clear, with the cells well arranged; however, compared to the control, the outer and nuclear layers of the retina of the 10,000 lux group became thinner, and the cells in the retinas of the 15,000 and 20,000 lux groups were missing (Figure 1).

Blue light exposure triggers dysfunction of the retina: To investigate the influence of blue light exposure on retina function, the mice were exposed to blue light for 5 days (8 h/day), and ERG was performed. Light intensities of 10,000, 15,000, and 20,000 lux were chosen. Five days after modeling, ERG showed that the a- and b-wave amplitudes of the blue light exposure group were significantly decreased by 0.5–2.0 fold, respectively (Figure 2).

Blue light exposure induces cell death of the retina: To investigate the influence of blue light exposure on cell

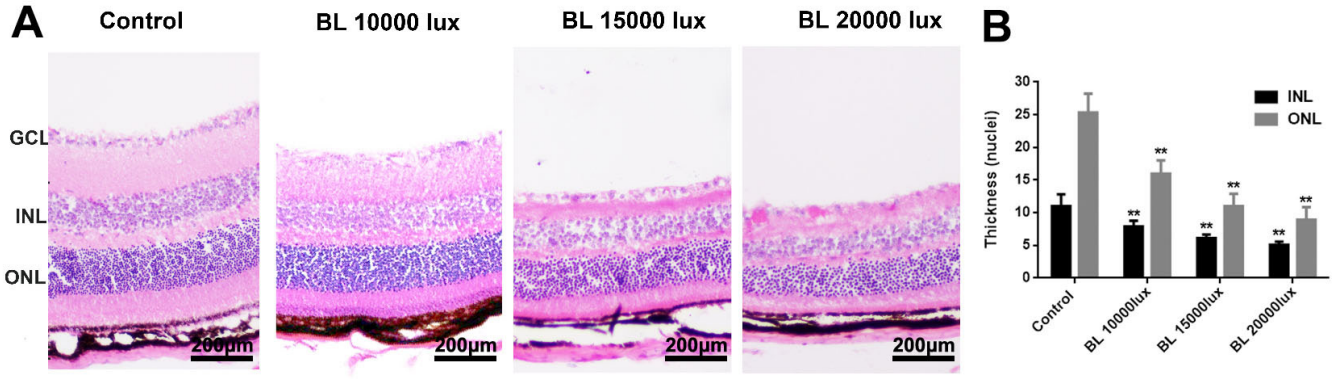

Figure 1. The effect of blue light exposure on the structure of the retina in C57BL/6J mice. C57BL/6J mice were exposed to different intensities of blue light (10,000, 15,000, and 20,000 lux) for 5 days (8 h/day), and hematoxylin–eosin (HE) staining was used to evaluate the structure of the mouse retina. INL: inner nuclear layer, ONL: outer nuclear layer, GCL: ganglion cell layer. **p<0.001.

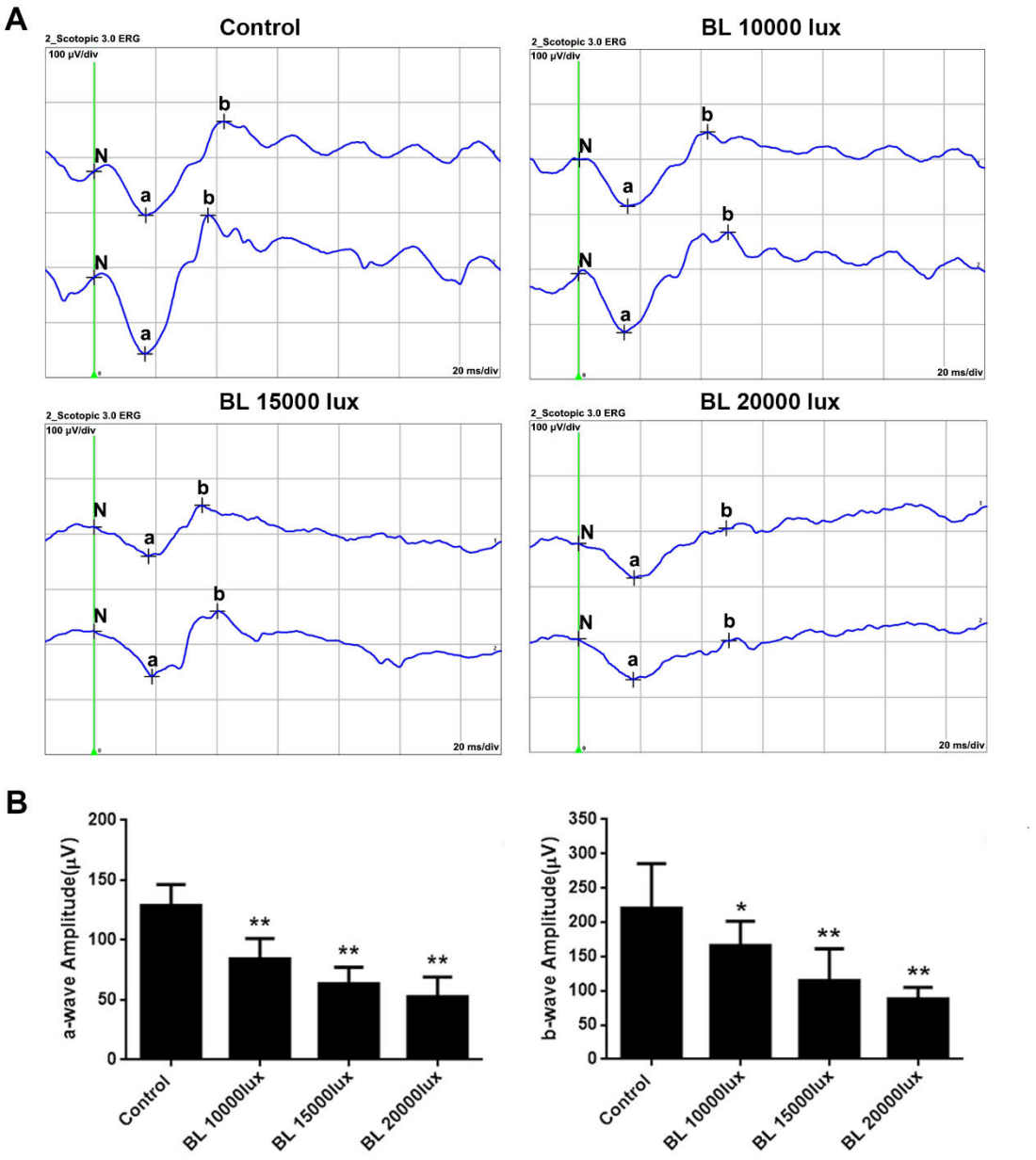

Figure 2. The effect of blue light exposure on the function of the retina in C57BL/6J mice. C57BL/6J mice were exposed to different intensities of blue light (10,000, 15,000, and 20,000 lux) for 5 days (8 h/day), and electroretinography (ERG) was used to evaluate the function of the mouse retina. **A**: Representative diagram of the electroretinogram. **B**: Statistical analysis of the ERG (a- and b-waves) data in different groups. The data were analyzed in the form of mean ± standard deviation (SD; n = 3) with left and right eyes separately. *p<0.05, **p<0.01 versus the control group.

death, the mice were exposed to blue light for 5 days (8 h/day), and TUNEL assay was performed. Light intensities of 10,000, 15,000, and 20,000 lux were chosen. Five days after modeling, a small number of apoptotic bodies were found in the outer nuclear layer (ONL) with 10,000 lux light intensity, and a large number of apoptotic bodies were detected in the ONL with 15,000 and 20,000 lux (Figure 3). Under severe conditions, cell death but not inflammation is the main hallmark. The 10,000 lux light intensity was chosen for in vivo model construction in the subsequent experiments for inflammation evaluation.

Micro-PET imaging and biodistribution of the BL mice model: Micro-PET imaging of [^{18}F]-DPA-714 was used to evaluate the inflammatory status of the retina in the BL mice model,

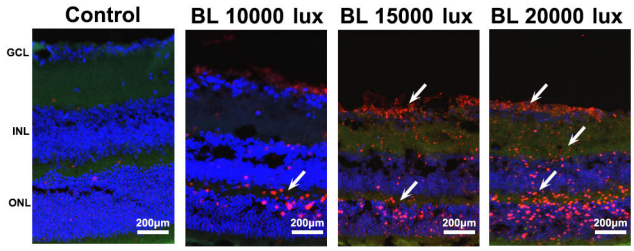

Figure 3. The effect of blue light exposure on the cell death of the retina in C57BL/6J mice. C57BL/6 mice were exposed to different intensities of blue light (10,000, 15,000, and 20,000 lux) for 5 days, and terminal-deoxynucleotidyl transferase 24 (TdT)-mediated nick-end labeling (TUNEL) assay was used to evaluate the cell death of the mouse retinas (TUNEL: red fluorescence, 2-(4-Amidinophenyl)-6-indolecarbamidine dihydrochloride [DAPI]: blue fluorescence). INL: inner nuclear layer, ONL: outer nuclear layer, GCL: ganglion cell layer.

and a light intensity of 10,000 lux was chosen. Five days after modeling, the uptake of [^{18}F]-DPA-714 in the eyeballs of the mice exposed to blue light was significantly upregulated compared to the controls (Figure 4A). In addition, region of interest (ROI) analysis showed that eyeball uptake in the BL group and the control group was 2.133±0.0121 ID%/g (n = 6) and 1.492±0.1961 ID%/g (n = 6; p<0.0001), respectively (Figure 4B). Then, the biodistribution data showed that the uptake of the retinal and choroidal layers in the eye was higher in the mice exposed to blue light, indicating that the expression of TSPO was significantly increased in the retina and the choroid under blue light exposure (Figure 4C). Corneal uptake in the BL group and the control group was 1.60±0.1372 ID%/g (n = 6) and 0.69±0.2031 ID%/g (n = 6; p < 0.001), retinal uptake in the BL group and the control group was 3.13±0.1581 ID%/g (n = 6) and 1.32±0.1808 ID%/g (n = 6; p<0.0001), and choroid uptake in the BL group and the control group was 3.33±0.1213 ID%/g (n = 6) and 1.88±0.1621 ID%/g (n = 6; p<0.0001). The uptake by the cornea, retina, and choroid was significantly different between the BL group and the control group, and the change in the [^{18}F]-DPA-714 uptake in the retina was the highest.

TSPO expression in retinal microglial cells of the BL mice model: Microglial TSPO is the target of DPA-714, and its expression was further analyzed in a BL mice model. Light intensity of 10,000 lux was chosen. Five days after modeling, the expression of TSPO was significantly upregulated and migrated from the inner nuclear layer (INL) to the ONL using IHC (Figure 5A). Then, TSPO was identified as the main marker of microglia in the retina, and it colocated with microglia (Figure 5B). The results indicated that the inflammatory status of the retina occurred at the early stage of blue light injury and was consistent with the micro-PET imaging data (Figure 5C).

DISCUSSION

The translocator protein (18 kDa; TSPO), a biomarker of brain microgliosis, has been introduced as a possible molecular target for peripheral sterile inflammatory disease PET imaging [23]. PET imaging of this protein may address disease heterogeneity, assist in patient stratification, and contribute to predicting treatment response [24]. A previous study showed that TSPO is highly expressed in microglia of degenerating retinas [25]. In this study, using mice exposed to blue light as an in vivo model of AMD, we found that TSPO was significantly upregulated in the retinal microglia of mice with BL 10,000 lux exposure, and micro-PET imaging based on [^{18}F]-DPA-714 indicated the inflammatory status of the retina early in vivo.

[^{18}F]-DPA-714 is a second-generation TSPO positron emission tomography radiotracer that shows great promise in a model of acute neuroinflammation [26]. Using [^{18}F]-DPA-714 PET, Sanhita et al. documented in vivo neuroinflammatory changes in the brain with disruption of the blood–brain barrier [27]. Liu et al. investigated the influences of light therapy on microglial activation in the brains of depressive rats using [^{18}F]-DPA-714 PET [28]. Géraldine et al. demonstrated that [^{18}F]-DPA-714 is adapted to monitor in vivo inflammatory processes in an rheumatoid arthritis (RA) experimental model [29]. Using diabetic retinopathy (DR) rats as an in vivo model, Zhou et al. found that [^{18}F]-DPA-714 PET/CT appears to be a useful noninvasive imaging method for detecting TSPO in the retina [30]. In this study, HE staining, ERG, and TUNEL assay revealed that blue light could induce retinal injury with structural destruction and neuronal cell death, and its severity depended on the light intensity, exposure duration, and wavelength. By choosing low light intensity, we found that the SUVmean of [^{18}F]-DPA-714 was markedly enhanced in the eyeballs of BL mice compared with that of normal controls after 5 days of BL 10,000 lux exposure. The SUVmean of ROIs in the eyeballs of the BL

and control mice was 2.133 ID%/g (n = 6) and 1.492 ID%/g(n = 6; p<0.0001), respectively. Biologic distribution analysis showed there were significant differences in the uptake by the cornea, retina, and choroid between the blue light group and the control group. The overall [^{18}F]-DPA-714 uptake of the eyeball except vitreous body was significantly increased, and the change in the [^{18}F]-DPA-714 uptake were most obvious in the retina. In addition, the uptake of [^{18}F]-DPA-714 in the heart, liver, spleen, lung, and kidney was similar between the two groups, indicating blue light affected only the expression of TSPO in eyeball. Furthermore, to confirm the expression of TSPO in the retina, the mice were immediately killed after micro-PET imaging, and IHC, IFC, and western blotting were used to evaluate the expression level of TSPO in the retina. IHC and western blotting showed TSPO was significantly upregulated in the retina under blue light exposure. IFC showed that microglia were activated under blue light exposure and were colocalized with TSPO, indicating that the upregulation of TSPO mainly depended on the activation of microglia.

In conclusion, based on the results above, we concluded that TSPO was significantly upregulated in retinal microglia under a low intensity of blue light exposure, and [^{18}F]-DPA-714 micro-PET imaging is a good alternative for evaluating the inflammatory status of the retina under pathological process. However, further investigation regarding the early diagnostic value of [^{18}F]-DPA-714 micro-PET imaging for retinal inflammation needs to be conducted in a time-dependent manner.

ACKNOWLEDGMENTS

The present study was supported by Six talent peaks project in Jiangsu Province (WSW-047), Six-one Scientific Research Project (LGY2019087), Young Talent's Subsidy Project in Science and Education of the Department of Public Health of Jiangsu Province (QNRC2016627) and Project of Wuxi Health Commission (Z202009, Z202110). Author Contribution Yuan Chen, Ke Wang and Min Yang designed the study and performed the in vitro and in vivo work. Yixiang Zhou

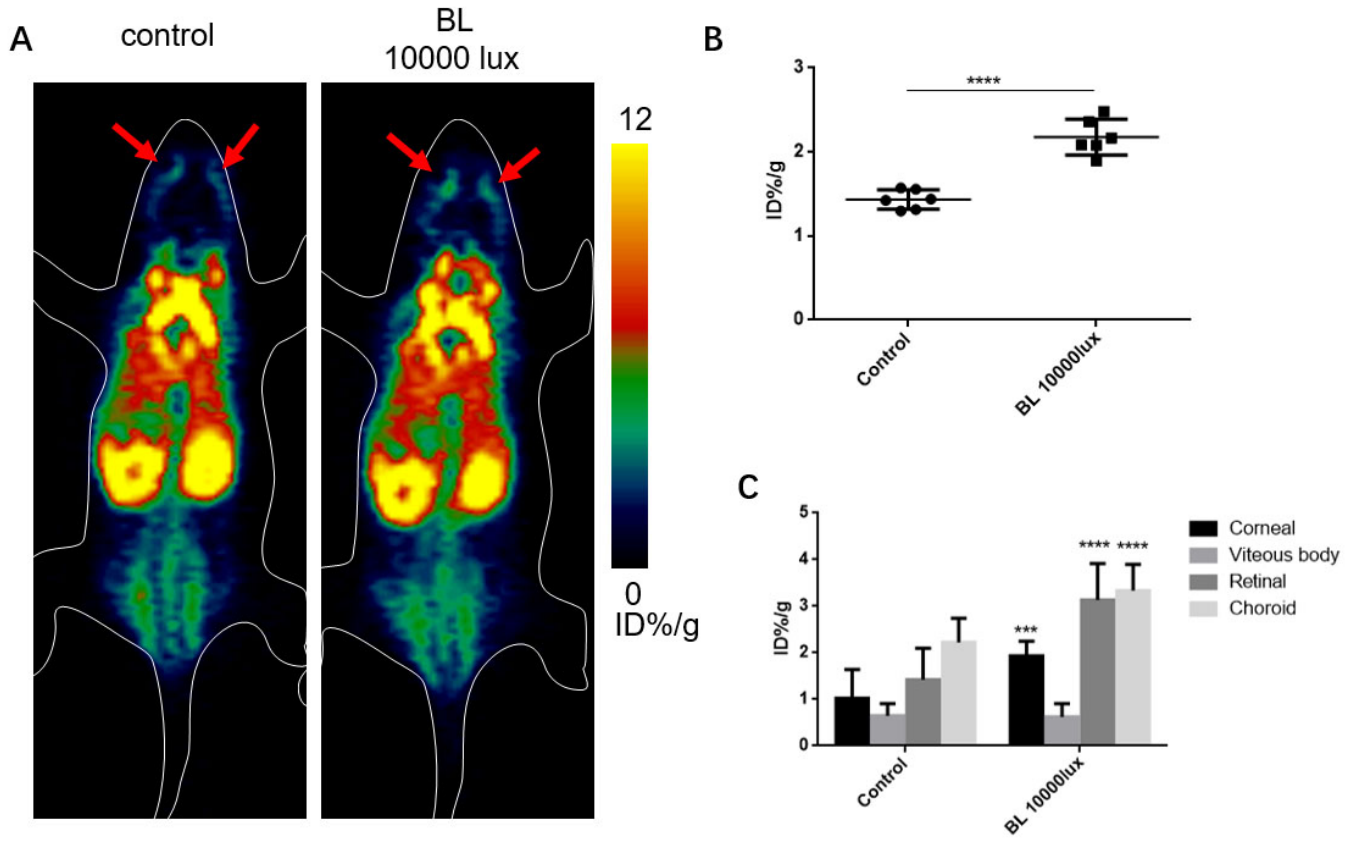

Figure 4. PET images of [^{18}F]-DPA-714 were used to evaluate the systemic inflammatory state of blue light–injured mice. **A**: Micro-positron emission tomography (PET) whole-body image of the control and blue light–damaged mice. **B**: Blue light–damaged mice average ID%/g of eyeballs. ****p<0.0001 versus control group. **C**: Biodistribution of the cornea, vitreous body, retina, and choroid was assessed by analyzing the mean ID%/g. ***p<0.001, ****p<0.0001 versus the control group.

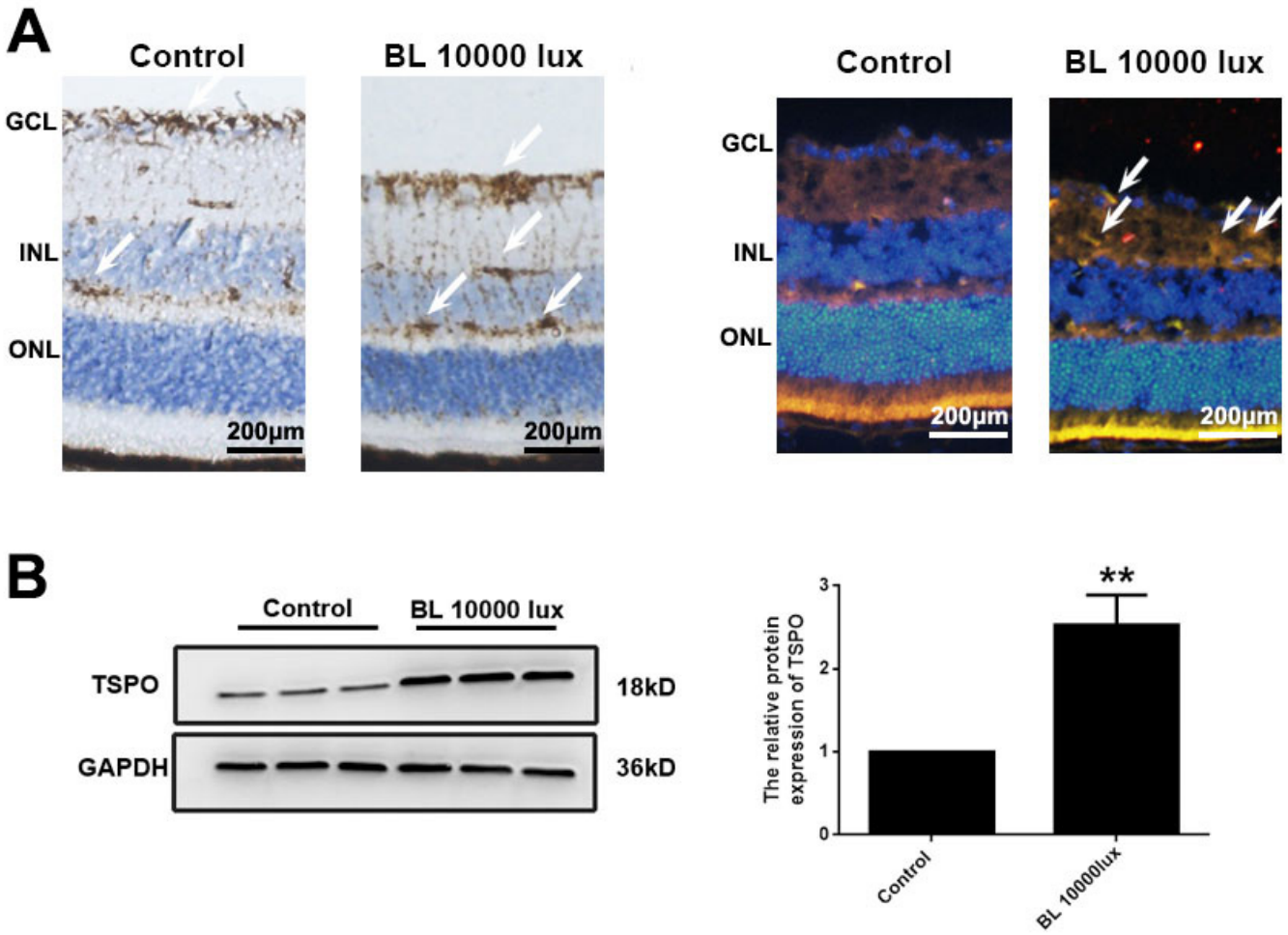

Figure 5. The expression of TSPO in normal retina and blue light–damaged retina. **A**: The expression and location of translocator protein (TSPO) were analyzed with immunohistochemical staining. **B**: Immunofluorescence staining of the retinal slices. (TSPO: red fluorescence, IBA-1 (a microglia marker): green fluorescence, 2-(4-Amidinophenyl)-6-indolecarbamidine dihydrochloride (DAPI): blue fluorescence). **C**: The expression of TSPO in the retina was analyzed with western blotting. **p<0.01 versus the control group. INL: inner nuclear layer, ONL: outer nuclear layer, GCL: ganglion cell layer.

and Donghui Pan participated in the in vivo work. Ge Yan scored the immu-nostains. Yuan Chen wrote the manuscript; Lizhen Wang, Ke Wang and Min Yang contributed to writing and editing the manuscript. Dr. Yang (yangmin@jsinm.org) and Dr. Wang (wangke@jsinm.org) are co-corresponding authors.

REFERENCES

1. Jonas JB, Cheung CMG, Panda-Jonas S. Updates on the Epidemiology of Age-Related Macular Degeneration. Asia Pac J Ophthalmol (Phila) 2017; 6:493-7. [PMID: 28906084].
2. Garcia-Layana A, Cabrera-Lopez F, Garcia-Arumi J, Arias-Barquet L, Ruiz-Moreno JM. Early and intermediate age-related macular degeneration: update and clinical review. Clin Interv Aging 2017; 12:1579-87. [PMID: 29042759].
3. Francisco SG, Smith KM, Aragones G, Whitcomb EA, Weinberg J, Wang X, Bejarano E, Taylor A, Rowan S. Dietary Patterns, Carbohydrates, and Age-Related Eye Diseases. Nutrients 2020; 12:2862-[PMID: 32962100].
4. Pennington KL, DeAngelis MM. Epidemiology of age-related macular degeneration (AMD): associations with cardiovascular disease phenotypes and lipid factors. Eye Vis (Lond) 2016; 3:34-[PMID: 28032115].
5. Alaimo A, Linares GG, Bujjamer JM, Gorojod RM, Alcon SP, Martinez JH, Baldessari A, Grecco HE, Kotler ML. Toxicity of blue led light and A2E is associated to mitochondrial dynamics impairment in ARPE-19 cells: implications for age-related macular degeneration. Arch Toxicol 2019; 93:1401-15. [PMID: 30778631].
6. Anderson DH, Radeke MJ, Gallo NB, Chapin EA, Johnson PT, Curletti CR, Hancox LS, Hu J, Ebright JN, Malek G, Hauser MA, Rickman CB, Bok D, Hageman GS, Johnson LV.

The pivotal role of the complement system in aging and age-related macular degeneration: hypothesis re-visited. Prog Retin Eye Res 2010; 29:95-112. [PMID: 19961953].

7. Wielgus AR, Collier RJ, Martin E, Lih FB, Tomer KB, Chignell CF, Roberts JE. Blue light induced A2E oxidation in rat eyes–experimental animal model of dry AMD. Photochem Photobiol Sci 2010; 9:1505-12. .

8. Xie T, Cai J, Yao Y, Sun C, Yang Q, Wu M, Xu Z, Sun X, Wang X. LXA4 protects against blue-light induced retinal degeneration in human A2E-laden RPE cells and Balb-c mice. Ann Transl Med 2021; 9:1249-[PMID: 34532386].

9. Wechalekar K, Sharma B, Cook G. PET/CT in oncology–a major advance. Clin Radiol 2005; 60:1143-55. [PMID: 16223611].

10. Bauer M, Karch R, Tournier N, Cisternino S, Wadsak W, Hacker M, Marhofer P, Zeitlinger M, Langer O. Assessment of P-Glycoprotein Transport Activity at the Human Blood-Retina Barrier with (R)-(11)C-Verapamil PET. J Nucl Med 2017; 58:678-81. [PMID: 27738009].

11. Caravaggio F, Scifo E, Sibille EL, Hernandez-Da Mota SE, Gerretsen P, Remington G, Graff-Guerrero A. Expression of dopamine D2 and D3 receptors in the human retina revealed by positron emission tomography and targeted mass spectrometry. Exp Eye Res 2018; 175:32-41. [PMID: 29883636].

12. Kashani AH, Asanad S, Chan JW, Singer MB, Zhang J, Sharifi M, Khansari MM, Abdolahi F, Shi Y, Biffi A, Chui H, Ringman JM. Past, present and future role of retinal imaging in neurodegenerative disease. Prog Retin Eye Res 2021; 83:100938-[PMID: 33460813].

13. De Picker LJ, Haarman BCM. Applicability, potential and limitations of TSPO PET imaging as a clinical immunopsychiatry biomarker. Eur J Nucl Med Mol Imaging 2021; 49:164-73. [PMID: 33735406].

14. Herschman HR. Micro-PET imaging and small animal models of disease. Curr Opin Immunol 2003; 15:378-84. [PMID: 12900267].

15. Auso E, Gomez-Vicente V, Esquiva G. Biomarkers for Alzheimer's Disease Early Diagnosis. J Pers Med 2020; 10:114-[PMID: 32899797].

16. Lambert NG, ElShelmani H, Singh MK, Mansergh FC, Wride MA, Padilla M, Keegan D, Hogg RE, Ambati BK. Risk factors and biomarkers of age-related macular degeneration. Prog Retin Eye Res 2016; 54:64-102. [PMID: 27156982].

17. Biswas L, Ibrahim KS, Li X, Zhou X, Zeng Z, Craft J, Shu X. Effect of a TSPO ligand on retinal pigment epithelial cholesterol homeostasis in high-fat fed mice, implication for age-related macular degeneration. Exp Eye Res 2021; 208:108625-[PMID: 34022174].

18. Rodríguez-Chinchilla T, Quiroga-Varela A, Molinet-Dronda F, Belloso-Iguerategui A, Merino-Galan L, Jimenez-Urbieta H, Gago B, Rodriguez-Oroz MC. [(18)F]-DPA-714 PET as a specific in vivo marker of early microglial activation in a rat model of progressive dopaminergic degeneration. Eur J Nucl Med Mol Imaging 2020; 47:2602-12. [PMID: 32206840].

19. Kuszpit K, Hollidge BS, Zeng X, Stafford RG, Daye S, Zhang X, Basuli F, Golden JW, Swenson RE, Smith DR, Bocan TM. [(18)F]DPA-714 PET Imaging Reveals Global Neuroinflammation in Zika Virus-Infected Mice. Mol Imaging Biol 2018; 20:275-83. [PMID: 28900831].

20. Zhou Y, Ou Y, Ju Z, Zhang X, Zheng L, Li J, Sun Y, Liu X. Visualization of translocator protein (18 kDa) (TSPO) in the retina of diabetic retinopathy rats using fluorine-18-DPA-714. Ann Nucl Med 2020; 34:675-81. [PMID: 32632564].

21. Tang D, Hight MR, McKinley ET, Fu A, Buck JR, Smith RA, Tantawy MN, Peterson TE, Colvin DC, Ansari MS, Nickels M, Manning HC. Quantitative preclinical imaging of TSPO expression in glioma using N,N-diethyl-2-(2-(4-(2–18F-fluoroethoxy)phenyl)-5,7-dimethylpyrazolo[1,5-a]pyrimidin-3-yl)acetamide. J Nucl Med 2012; 53:287-94. [PMID: 22251555].

22. Zhu C, Xu Q, Pan D, Xu Y, Liu P, Yang R, Wang L, Sun X, Luo S, Yang M. Prostate cancer imaging of FSHR antagonist modified with a hydrophilic linker. Contrast Media Mol Imaging 2016; 11:99-105. [PMID: 26286841].

23. Barresi E, Robello M, Costa B, Da Pozzo E, Baglini E, Salerno S, Da Settimo F, Martini C, Taliani S. An update into the medicinal chemistry of translocator protein (TSPO) ligands. Eur J Med Chem 2021; 209:112924-[PMID: 33081988].

24. Scholz R, Caramoy A, Bhuckory MB, Rashid K, Chen M, Xu H, Grimm C, Langmann T. Targeting translocator protein (18 kDa) (TSPO) dampens pro-inflammatory microglia reactivity in the retina and protects from degeneration. J Neuroinflammation 2015; 12:201-[PMID: 26527153].

25. Wolf A, Herb M, Schramm M, Langmann T. The TSPO-NOX1 axis controls phagocyte-triggered pathological angiogenesis in the eye. Nat Commun 2020; 11:2709-[PMID: 32483169].

26. Sridharan S, Lepelletier FX, Trigg W, Banister S, Reekie T, Kassiou M, Gerhard A, Hinz R, Boutin H. Comparative Evaluation of Three TSPO PET Radiotracers in a LPS-Induced Model of Mild Neuroinflammation in Rats. Mol Imaging Biol 2017; 19:77-89. [PMID: 27481358].

27. Sinharay S, Tu TW, Kovacs ZI, Schreiber-Stainthorp W, Sundby M, Zhang X, Papadakis GZ, Reid WC, Frank JA, Hammoud DA. In vivo imaging of sterile microglial activation in rat brain after disrupting the blood-brain barrier with pulsed focused ultrasound: [18F]DPA-714 PET study. J Neuroinflammation 2019; 16:155-[PMID: 31345243].

28. Liu Y, Wang L, Pan D, Li M, Li Y, Wang Y, Xu Y, Wang X, Yan J, Wu Q, Lu L, Yuan K, Yang M. PET evaluation of light-induced modulation of microglial activation and GLP-1R expression in depressive rats. Transl Psychiatry 2021; 11:26-[PMID: 33414373].

29. Pottier G, Bernards N, Dollé F, Boisgard R. [^{18}F]DPA-714 as a biomarker for positron emission tomography imaging of rheumatoid arthritis in an animal model. Arthritis Res Ther 2014; 16:R69-[PMID: 24621017].

30. Zhou Y, Ou Y, Ju Z, Zhang X, Zheng L, Li J, Sun Y, Liu X. Visualization of translocator protein (18 kDa) (TSPO) in the

retina of diabetic retinopathy rats using fluorine-18-DPA-714. Ann Nucl Med 2020; 34:675-81. [PMID: 32632564].